

Scalability of Hybrid-Electric Propulsion for VTOL UAS

Michael Avera **Rajneesh Singh**

U.S. Army Combat Capabilities Development Command, Army Research Lab
Aberdeen Proving Ground, MD
UNITED STATES OF AMERICA

michael.p.avera.civ@mail.mil rajneesh.k.singh.civ@mail.mil

Keywords: VTOL UAS, Electric-Hybrid, Design, Propulsion, Vehicle-configuration

ABSTRACT

This paper investigates scalability of electric propulsion architectures on the performance of vertical lift UAS to determine appropriate propulsion system designs at different vehicle scales. The HYDRA rotorcraft design code is used to size a quad-rotor biplane tailsitter UAV with five different electrical, mechanical, and hybrid propulsions system configurations. The scaling characteristics of each configuration is demonstrated by varying the payload and distance of the payload delivery mission. For 5 lb payloads and a mission distance of 35 nmi, the battery-electric configuration has the lowest takeoff weight and the highest energy specific delivery productivity. For 50 lb payloads, the fuel-burning mechanical propulsion configuration has the lowest takeoff weight and highest productivity. At higher payloads, the battery-electric design fails to converge to feasible designs and is observed to be highly sensitive to the wing weight estimate. Energy specific productivity doubles for the fuel burning designs due to significantly higher gravimetric energy density of fuel compared to batteries.

1.0 INTRODUCTION

The U.S. Army identified Vertical Take Off and Landing (VTOL) Unmanned Aerial Systems (UAS) as having an important role in the future of Army aviation (US Army UAS Center of Excellence, 2010). Several new and improved capabilities are expected to be enabled by autonomous UAS platforms, as envisaged in the Army's Multi-Domain Operation concept (TRADOC, 2018). Additional UAS applications may include aerial resupply; intelligence, surveillance, and reconnaissance (ISR); electronic attack; and advanced teaming with manned and unmanned systems. The diverse set of missions with varying emphasis on performance attributes (speed, range, payload, acoustics signature, maneuverability etc) for the UAS necessitates design and development of innovative vehicle configurations.

Vehicle configuration and propulsion system architecture are two key drivers for vehicle performance attributes. The two are interconnected in the sense that the chosen vehicle configuration imposes constraints on the design space of the propulsion architecture and vice versa. However, the propulsion system can be studied independently and derive valuable lessons for a broad category of UAS platforms. The focus of this paper is to explore scalability of different propulsion system architectures including hybrids and their scaling attributes. Both energy density and power density are important considerations for the propulsion systems. Energy density is a measure of the energy in the fuel and the conversion efficiency of the power converter (engine). Power density is a measure of the power converter. For example, the propulsion system weight of a long-range transport aircraft is dominated by the energy density of the fuel consumed (which may be 10 times the weight of the engines). In contrast, a solar-powered vehicle has zero fuel weight and, thus, very high energy density but low power density (the solar cells and power storage system are heavy). VTOL UAS have a unique power requirement profile where the power required can be significantly different for the hover and cruise flight segments. The goal of the hybrid-electric propulsion system is to exploit inherent advantages of different propulsion technologies to achieve high power to weight ratios across the flight

regimes.

The vehicle configuration analyzed for this research effort is the quad-rotor biplane tailsitter. This configuration consists of four rotors arranged similar to a traditional quad-rotor with the addition of a wing underneath each pair of rotors. The addition of the wings enables the vehicle to pitch forward 90 degrees in forward flight and utilize the more efficient wings to generate lift in forward flight, thus increasing the range and utility of the vehicle. This axial flight orientation also allows the propeller speed to be reduced, significantly lowering the power consumption rate. Researchers at the U.S. Army Combat Capabilities Development Command (CCDC) Army Research Laboratory recently launched a collaborative initiative to investigate knowledge and technology gaps common to VTOL UAS platforms (Singh, Sirohi, & Hrishikeshvan, 2019). The Common Research Configuration (CRC) represents a family of quad-rotor biplane tailsitter UAS vehicles that span Group 1 to Group 3 size classes. The 20 lb CRC-20 and the 2.5 lb CRC-3 are pictured in. The CRC-20 is the objective vehicle size from which a number of initial research tasks will be conducted in the areas of advanced flight controls, acoustic predictions, interactional



Figure 1.1-1 Army Research Lab's CRC-20 (top) and CRC-3 (bottom) quad-rotor biplane tailsitter UAVs.

aerodynamics, and vehicle performance and weight predictions.

1.1 Propulsion Architectures

The primary goal of this paper is to explore the mission capabilities and scaling effects of a UAV with electrical, mechanical, and hybrid propulsion architectures. To do so, five separate vehicles will be designed using a VTOL aircraft design code incorporating the propulsion architectures listed in Table 1. For each propulsion architecture, a new vehicle will be sized to complete a payload delivery mission of varying range.

The first propulsion system configuration is a traditional all-electric architecture commonly seen on commercial off-the-self (COTS) quad-rotors and is shown in. It is the simplest configuration due to a low number of subsystem components and control inputs (only requires 4 rotor speeds). Its biggest disadvantage is typically limited endurance due to low specific energy batteries.

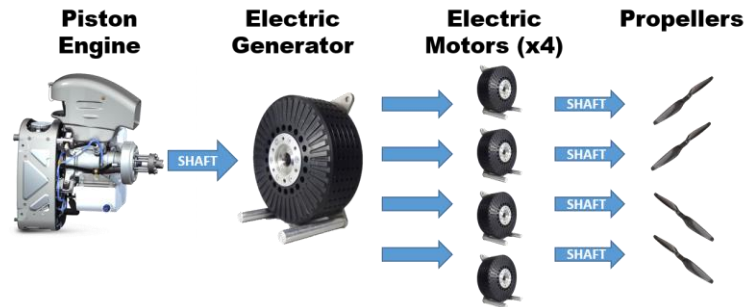


Figure 1.1-4 Propulsion system configuration #3 is an electric transmission system. The electric generator converts mechanical energy from the fuel burning piston engine into electrical energy supplied to the four electric motors and fixed pitch rotors.

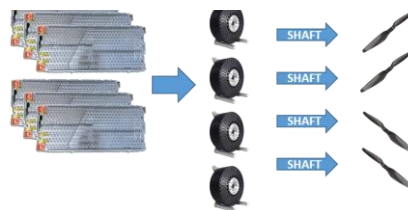


Figure 1.1-3 Propulsion system configuration #1 is an all electric drivetrain. Energy is stored by a battery and consumed by 4 electric motors.

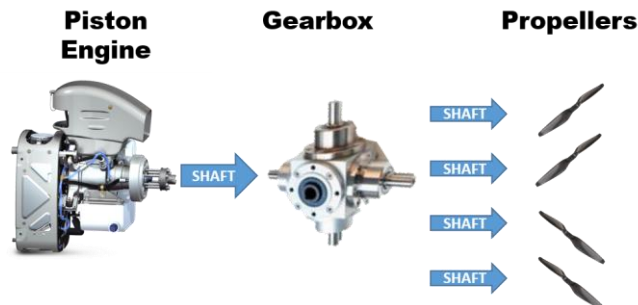


Figure 1.1-2 Propulsion system configuration #2 is a traditional mechanical drivetrain powered by a fuel burning piston engine which supplies power to the four rotors via a gearbox.

Configuration number 2 is a entirely mechanical propulsion system with a fuel burning internal combustion engine (ICE) powering all four rotors through a single dividing gearbox as shown in. Mechanical drive systems tend to be heavier than their electric counterparts due to increased weight from gearboxes, lubrication systems, and their scaling trends with torque requirements. This configuration uses variable pitch blades for primary flight control, similar to a traditional helicopter, instead of variable rotor speed used in the other configurations. so that one engine can drive all rotors.

Configuration number 3 is an electric transmission configuration as shown in. It replaces the battery in the full electric design for a fuel-burning engine, electric generator, and fuel tank. This configuration retains the variable speed electric motors for primary flight control. It is expected that this configuration will have a significantly longer range than battery powered designs due to the higher energy density of fuel compare to batteries. While it is expected that a vehicle of this type would be required to have a backup battery, such a battery is only utilized in emergency situations for this analysis and is not intended to be used for increasing the vehicle’s performance capabilities.

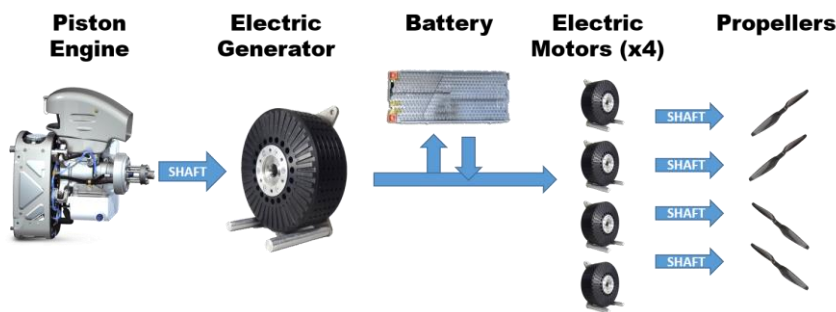


Figure 1.1-5 Propulsion system configuration #4 is a series hybrid arrangement with a battery. The battery provides a temporary increase in power in addition to the ICE

. The battery can provide a temporary increase in power available on top of the continuous power produced by the ICE. The battery can be sized to provide additional power situationally during hovering flight and to increase maximum dash speed. The dual energy sources allow the fuel-burning engine and electric generator to be sized for continuous and lower power required segments while the battery is sized for short duration high power segments.

Configuration number 5 is parallel hybrid arrangement as shown in. A fuel-burning engine and electric generator provide power to a single electric motor. Simultaneously, the ICE drives a gearbox which is mechanically linked to all four variable pitch rotors. The electric motor is connected to the gearbox input shaft. This configuration allows the aircraft to selectively utilize only the fuel burning engine, only the electric motor, or a combination of both to provide power. Similarly, to the series hybrid design, this can allow for both electrical and ICE subsystems to be sized for different power requirements.

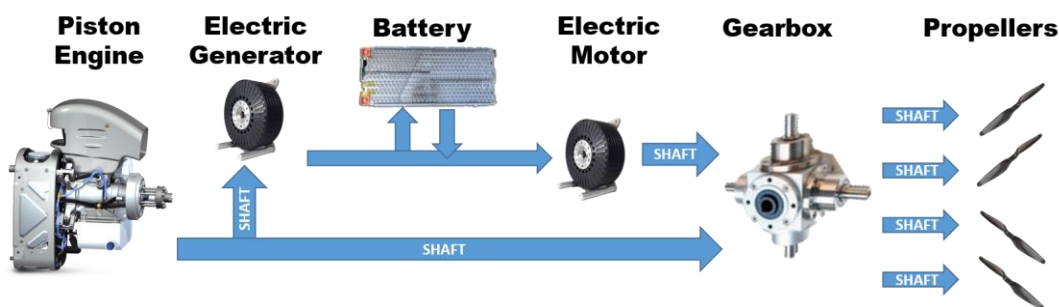


Figure 1.1-6 Propulsion system configuration #5 is parallel hybrid arrangement. The fuel burning engine powers an electric generator and a driveshaft which is connected to the four variable pitch propellers via a gearbox. An electrical generator charges a battery that supplies power to a single electric motor attached to the driveshaft.

1.2 Vehicle Sizing and Performance Analysis

While the goal of this paper is to understand the costs and benefits of various propulsion system architectures, the vehicle which these propulsion systems power must be designed and sized to account for the various architectures and to appropriately determine the thrust and power requirements during each segment of the mission. Studies which investigate hybrid propulsion systems (Ng, Patil, & Datta, 2019)

typically assume a fixed vehicle design and replace the chosen vehicle's propulsion system weight by the new hybrid system weight. While this method is sufficient for comparing the two propulsion systems, it does not allow for a thorough assessment of the new vehicles performance capabilities which are directly impacted by energy density and energy storage capacities. A comprehensive analysis resizes the entire vehicle (rotor, fuselage, and propulsion system) simultaneously.

To do so, this effort utilizes the HYbrid Design and Rotorcraft Analysis (HYDRA) rotorcraft sizing tool developed by researchers at the University of Maryland, College Park (UMD) in (Sridharan, Govindarajan, Nagaraj, & Chopra, 2016). HYDRA is a rotorcraft design and performance code, which generalizes the aircraft by defining locations of rotor, wing, fuselage, and propulsion subsystems and iteratively calculates mission power requirements and subsystem weights. The outputs are an aircraft definition that is optimal for completing the given mission and mission performance parameters such as energy used, payload vs range charts, and power curves.

HYDRA's framework facilitates the rapid assessment of a broad aircraft design space while providing means to successively increase the level of aerodynamic and structural analysis fidelity. This ensures feasible designs are discarded because of designer choice and not due to time or computational cost considerations. For example, a design space can be defined as a range of input values on multiple design parameters such as rotor disk loading, tip speed, wing aspect ratios, cruise RPM ratios, transmission efficiencies, and battery energy density. Using low fidelity methods such as momentum theory with a uniform inflow assumption, HYDRA can quickly assess the performance of 100,000's of design configurations for the given mission in a matter of 5—10 minutes. The user then selects a subset of those designs by narrowing the range of input parameters based on some measure of performance such as max speed, range, payload, and installed power. HYDRA can reassess this new subset of designs with a more rigorous BEMT or a rigid blade + free vortex wake analysis without requiring the use of an external code. These higher fidelity options allow blade geometry optimization to be performed during the initial design and sizing process. CPU and GPU technology have progressed enough such that comprehensive analysis and massive design space exploration are relatively quick to process and can be accommodated in the preliminary rotorcraft design process without significant increase in computation time. 7,000 cases can be run in approximately 2.5 hrs with a free-vortex wake model.

The HYDRA sizing tool also makes an effort to more accurately predict blade weight and fuselage weight by using physics-based methods as described in (Govindarajan, Sridharan, & Avera, 2017) instead of traditional methods based on statistical regressions of historic VTOL aircraft subsystem weights. The error in predicting subsystem weights for Group 2 and Group 3 UAS with statistical models such as the AFDD00 weights models can be partially attributed to the size of the full-scale rotorcraft from which they were derived. These statistical models are not applicable to the smaller size of the Group 2 and Group 3 classes of UAVs. Recent efforts (Russell, Theodore, & Sekula, 2018) have been made to incorporate component weight trends and wind tunnel test data into rotorcraft design tools such as NDARC. However, these models are still empirically derived and are not as applicable to unique UAV designs which incorporate wings or other novel component layouts. A physics-based method of estimating component weights for this design space is ideal to maintain robustness and applicability to new and novel designs.

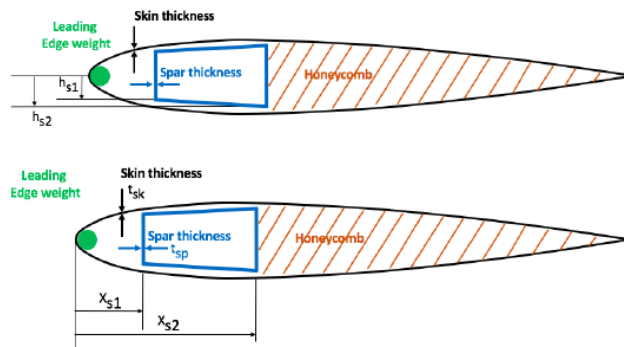
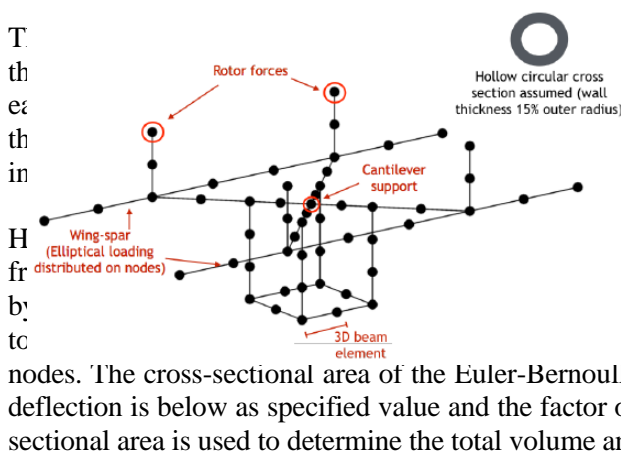


Figure 1.2-1 Nodal arrangement for quad-rotor biplane tailsitter used in HYDRA’s finite element analysis of UAV airframe weight (left) and physics-based blade and wing weight models (right).



parametrizing the blade cross-section using the skin geometry as shown in. Using known material properties, total stiffness is calculated. An optimization loop ensures each reach the yield stress of the subcomponents with an

each to estimate airframe weight. An example of this iteration is also shown in. The framework is constructed external loads are applied. The rotor forces are applied in an elliptical distribution along the wing spar nodes. The cross-sectional area of the Euler-Bernoulli beam elements are optimized such that the maximum deflection is below as specified value and the factor of safety is above a specified value. The resulting cross-sectional area is used to determine the total volume and weight of the airframe.

In (Avera, 2019) the effects of this physics-based approach to estimating airframe weight was applied to a quad-rotor, a tiltwing, and a quad-rotor biplane configuration. The physics-based models were able to capture a coupling between two competing design ideals, that larger rotors are more efficient and that more rotors on a single wing increases wing size and weight. The results showed that the tiltwing design required a compromise that is not apparent with the quad-rotor biplane and therefore had worse efficiency than the quad-rotor biplane tailsitter. This is but one example of the necessity for physics-based methods in vehicle design.

Table 2.0-1 List of aircraft parameters in aircraft design analysis.

Variable Parameters	
Rotor Disk Loading	1.0—5.0 lb/ft ²
Rotor Tip Speed (Hover)	150—250 ft/s
Rotor Tip Speed (Cruise)	0.4—1.0 * Hover Tip Speed
Wing Aspect Ratio	6—10
Wing Lift Coefficient	0.8—1.2
Blade Bilinear Twist	0—20 degrees
Blade Taper	1:1, 2:1, 3:1
Constant Parameters	
Battery Energy Density	158 W-hr/kg
Rotor induced power factor	1.178
Miscellaneous Weight	15%
Flat Plate Drag Factor	0.035

2.0 METHOD

For each payload size, 5 and 50 lb, a common payload delivery mission is used to size the quad-rotor biplane vehicle. The design space is defined by a range of values prescribed for the geometric and aerodynamic vehicle parameters listed in Table 2. For each combination of design parameters, a vehicle design is generated. The design with the lowest Gross Takeoff Weight (GTOW) is chosen as the optimum. The lightest designs for each of the five propulsion architectures are compared against each other for subsystem weights, mission energy consumption, and delivery efficiency. The optimal designs are also assessed against increasingly longer range missions to determine a trend of energy efficiency at each payload.

2.1 Propulsion System Models

Each propulsion system model consists of a combination of an ICE, electric motors, an electric generator, a gearbox, a battery, and a drive shaft. Each of these components has a parametric equation in HYDRA relating the component's weight to its operational requirements such as power, torque, and RPM. The details of each component model and their integration into the five propulsion architectures are described here.

2.1.1 Mechanical Drivetrain

The mechanical drivetrain consists of a gearbox which reduces the engine output shaft speed to a speed appropriate to the rotor. The output shaft of the gearbox is connected to a number of intermediate gearboxes which drive each rotor. The AFDD00 drive systems weight model from (Johnson, 2009) is used to estimate the weight of the gear boxes, rotor shafts, and drive shafts. This model accounts for number of rotors, drive shaft length, and system torque limit among other parameters to estimate the subsystem weight. The drive system efficiency is incorporated as a scalar factor of 0.85 applied to the output torque while the power output remains unchanged.

2.1.2 Piston Engine

The piston engine is represented by three main performance characteristics, weight, fuel consumption, and performance losses. The weight and specific fuel consumption (SFC) models are based on curve fits to data available from a database of aircraft piston engines with the smallest engine in the database being the Lycoming EL-005 single piston engine rated at 4hp max continuous power and 13.8 lb (6.25 kg) dry weight (Lycoming, n.d.). The SFC model considers each segment's power requirement in relation to the installed power or maximum power requirement for the entire mission. SFC remains relatively constant with altitude changes and all other losses such as engine efficiency and installation losses are captured by the database used for curve fitting.

2.1.3 Battery

The battery sizing model used in Hydra is shown in Equation 1. The battery is sized by arranging a number of battery cells in series, N_{SERIES} , to achieve the desired battery pack voltage, V_{BATT} . The battery voltage is determined by the maximum total voltage required by the electric motors throughout the mission. Then a number of these groups of cells are arranged in parallel, N_{PARALLEL} , to increase the total battery pack capacity, A_{BATT} which directly affects the duration of the battery discharge and the vehicles endurance. The discharge rate required, C_{RATE} , is determined by the maximum power required during the mission, P_{BATT} . Cells are assumed to have constant power output and are unaffected by variations in temperature and number of charge-discharge cycles. However, the maximum depth of discharge is limited to 85% to maintain adequate cell level output over a number of cycles. The pack's energy density of 158 W-hr/kg includes all extra weight incurred by cell management and cooling devices.

$$\begin{aligned}
 N_{SERIES} &= V_{BATT} / V_{CELL} \\
 A_{BATT} &= P_{BATT} / (V_{BATT} * C_{RATE}) \\
 N_{PARALLEL} &= \frac{A_{BATT}}{A_{CELL}} \\
 M_{BATT} &= M_{CELL} * N_{SERIES} * N_{PARALLEL}
 \end{aligned}
 \tag{1}$$

2.1.4 Electric Motor

Like the piston engine model, the weight of the electric motor is determined through curve fits of a database from available COTS Brushless Direct Current (BDC) electric motors. The electric motor efficiency is determined by scaling test data from a commonly available COTS BDC, the EMRAX 200 series (EMRAX). This efficiency map shown in is characteristic of typical BDC electric motor performance. It is important to capture this variation in motor efficiency due to changes in RPM because the propulsion configurations with variable RPM rotors can reduce rotor speed in forward flight and thus will operate at different motor efficiency than in hover. Electric motor efficiency using this method ranges from 86% to 96%.

2.1.5 Hybrid Drivesystems

The series hybrid drivetrain architecture is comprised of a piston engine which directly drives one electric generator. The electric generator directly powers all of the electric motors (configuration 3). An optional battery as is present in configuration 4 enables the piston engine to be sized for cruise flight while the battery augments the engine power for high power flight conditions such as hover as shown in Figure . This allows for the use of a smaller engine and trades engine weight for battery weight. 100% of the piston engine output shaft power is converted to electricity by the generator and there are no auxiliary drives or mechanisms to provide engine power directly to the rotors. The complete series hybrid drivesystem efficiency includes engine, generator and electric motor efficiency factors.

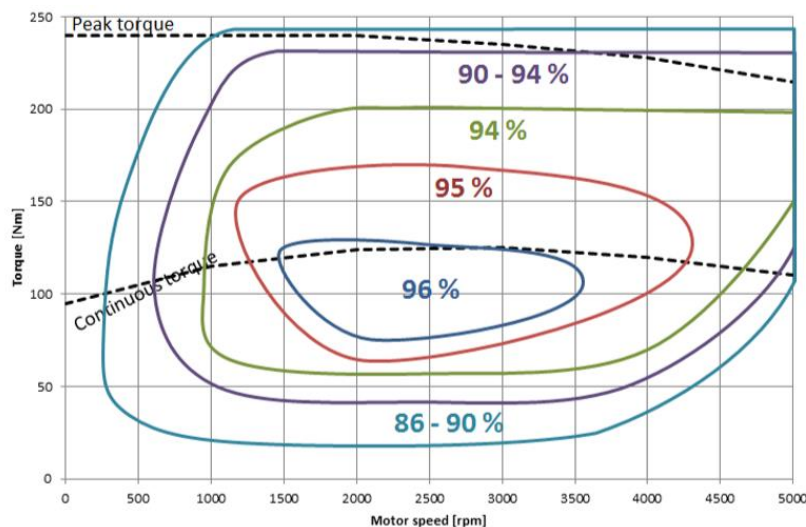


Figure 2.1.5-1 Electric motor efficiency map for EMRAX 228.

The parallel hybrid architecture model incorporates a mechanical drive system with an electric drivesystem. A single electric motor is connected to a common drive shaft which is then split by a gearbox to power each of the four propellers. The engine drives both a gearbox and an electric generator. The power split between

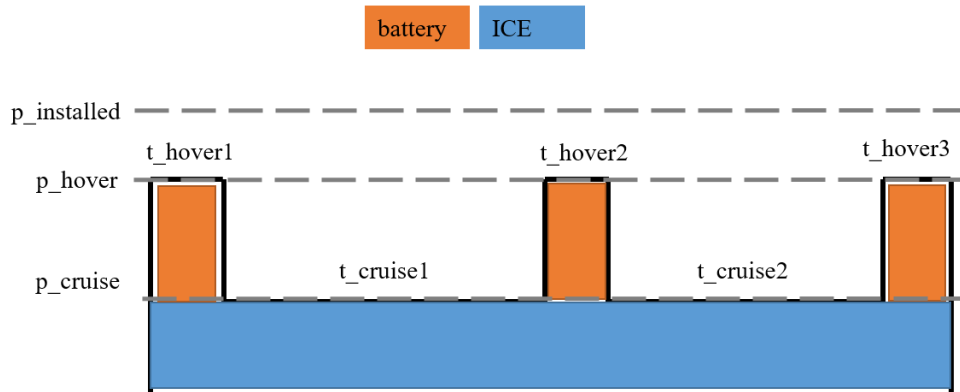


Figure 2.1.5-2 Example power sharing profile of hybrid electric propulsion system.

mechanical and electric drives can be selected based situationally.

2.1.6 Loads (BEMT rotor model)

Blade Element Momentum Theory (BEMT) is used to calculate power required and propeller efficiency of the rotors based on the thrust required after trimming the aircraft in steady level. BEMT discretizes the rotor blade into several sections which are assumed to act similar to 2D airfoils. Aerodynamic forces and moments are calculated via table lookup of lift, drag, and moment coefficients. Rotor performance is calculated by integrating the sectional loads along the span of the blade and again for an entire rotor revolution. BEMT equates the circulation theory of lift and momentum theory of lift and leads to a method of calculating rotor induced inflow during hover, axial climb, and edgewise forward flight conditions (Leishman, 2006).

Because of this discretized method, local changes in blade properties such as chord length and angle of attack (AoA) can be used to optimize the blade shape for best mission performance. For this effort, the blade shape properties that are varied are bilinear twist distribution (inboard twist, transition location, outboard twist), blade root pitch angle, and linear blade chord distribution (1:1, 2:1, 3:1 root to tip ratio). During the iterative aircraft sizing process, the BEMT method is an inner loop which calculates the performance of various rotor designs for the entire mission. The design which consumes the least amount of power to complete the mission is considered the optimal design. The Figure of Merit (FM) which relates the actual power required to the ideal power required and the rotor's propeller efficiency are used in the outer sizing loop for power calculations. The BEMT inner loop analysis is conducted for each iteration of the outer sizing loop as the vehicle design is updated.

3.0 RESULTS

Results are shown for each of the payload sizes considered by comparing the optimal design of the five propulsion architectures. Breakdowns of the vehicle subsystems show the variations in vehicle weight due to each propulsion design. Energy Specific Productivity (ESP) as defined in Equation 2 describes the vehicle's productivity of delivering payload weight over a distance per unit of energy consumed. More efficient designs have a higher ESP. This metric combines the data from the analyses into one metric which conveys the characteristics of each configuration and the design trade-offs among them.

$$Delivery\ Efficiency = \frac{Payload\ Weight\ (lb) * Range(nmi)}{Energy\ Consumed\ (HP - hr)} * \frac{HP - sec}{550\ ft - lb} * \frac{1\ hr}{3600\ sec} \quad (2)$$

3.1 5lb Payload

Figure 11 shows the comparison of the vehicle subsystem weights for each propulsion configuration when sized to the 5lb payload delivery mission. The all-electric configuration #1 weighs approximately 23 lb less than the next lightest design, the mechanical configuration #2. As expected, the battery-powered electric design is significantly more efficient than the others for carrying only a 5lb payload a distance of 35 nmi. Its much smaller GTOW suggests the vehicle will be the least costly to manufacture as cost typically scales with

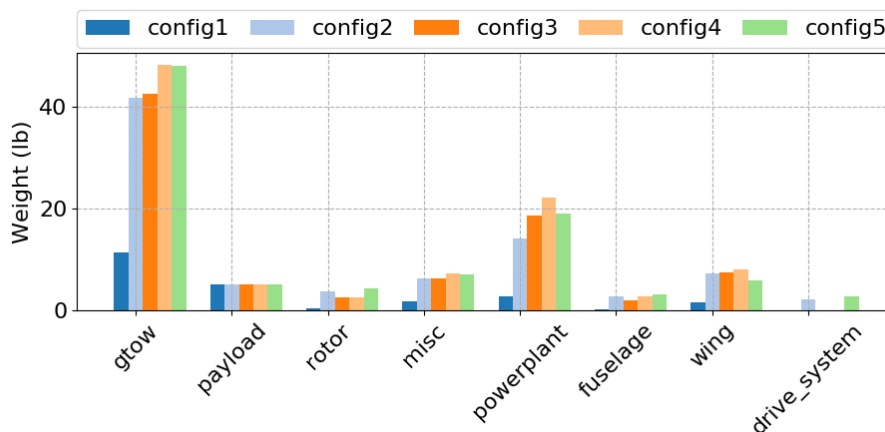


Figure 3.1-1 Subsystem weight breakdown for the UAVs with each of the 5 propulsion configurations sized for a 5lb payload delivery mission of 35nmi total range.

GTOW. While batteries do not provide nearly as high specific energy compared to hydrocarbon fuels, the engine and drivetrain necessary to extract energy by burning fuel weighs much more than the batteries for this scale. It should be noted that the smallest piston engine available in Hydra engine weight scaling model is the Lycoming EL-005. This engine weighs 14 lb which is almost the entire empty weight of the electric configuration for the 5lb payload mission. The lack of available certified engines below 14 lb is a significant impact on the minimum feasible weight of a piston engine powered design.

Of the three hybrid configurations, the electric transmission design weighed the least at 42.4 lb. The addition of the battery in the series hybrid system in configuration #4 increased the GTOW over configuration #3 by 5.8 lb. The series hybrid configuration #4 and the parallel hybrid configuration #5 both have approximately the same GTOW at about 48 lb.

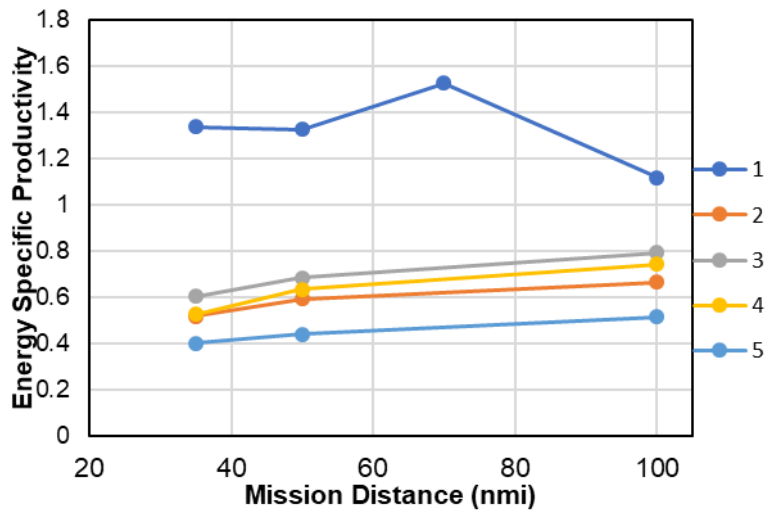


Figure 3.1-2 Productivity comparison of propulsion system architectures for varying mission distances with a 5lb payload.

Figure shows the comparison of delivery efficiency as defined by Equation 2 for all five configurations. Due to the significantly lighter GTOW, the all-electric configuration #1 has the most productivity per unit energy for all ranges assessed for the 5lb mission.

3.2 50lb Payload

Figure 12 shows the subsystem weight breakdown for the 50lb payload designs that are sized to the 35 nmi mission. The GTOW of all five designs ranged from 131—214 lb. The mechanically powered configuration #2 had the lowest GTOW of all designs, about 20% lower than the battery electric configuration #1, which was the lightest design for the previous 5lb payload mission. For the all-electric configuration, the battery alone was 23.8% of its GTOW.

Figure 13 shows the ESP of each configuration when sized to 35, 50 and 100 nmi mission ranges with the 50 lb payload. All designs with a combustion engine, configurations 2—5, nearly doubled in delivery efficiency while the battery-electric configuration #1 only increased delivery efficiency by 7% for the 35 nmi mission.

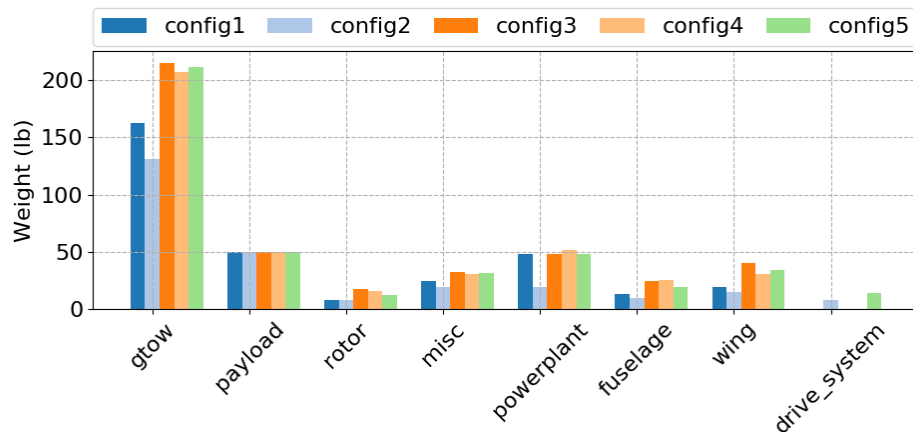


Figure 3.2-1 Subsystem weight breakdown for the UAVs with each of the 5 propulsion configurations sized for a 50lb payload delivery mission of 35nmi total range.

This highlights a key scaling characteristic of battery-electric designs which is that vehicles using batteries for primary energy storage have a much higher GTOW sensitivity to power requirements (e.g. payload) and mission distance or endurance than fuel-burning designs. The battery-electric configuration #1 had a relatively constant propulsion system weight fraction between the 5 lb and 50 lb missions of 42.3% and 42.7% respectively. However, the fuel-burning mechanical configuration #2 resulted in a 14.5% decrease in the fuel + propulsion system weight fraction from 40% in the 5 lb mission to 24% in the 50 lb mission. This suggests that fuel burning configurations are superior for larger payload requirements.

Hydra was unable to converge the battery-electric configuration #1 to a feasible design for missions longer than 40 nmi. It was observed that very high wing lift coefficients were necessary to converge on a solution, albeit a purely numerical one. The wing area is sized to the minimum necessary to achieve trimmed flight at the prescribed cruise speed and is driven primarily by lift coefficient. Hydra was able to successfully converge on a feasible design when the AFDD00 empirical trend was used to estimate wing weight instead of the physics-based method. The AFDD00 typically under predicts wing weight for smaller aircraft. This

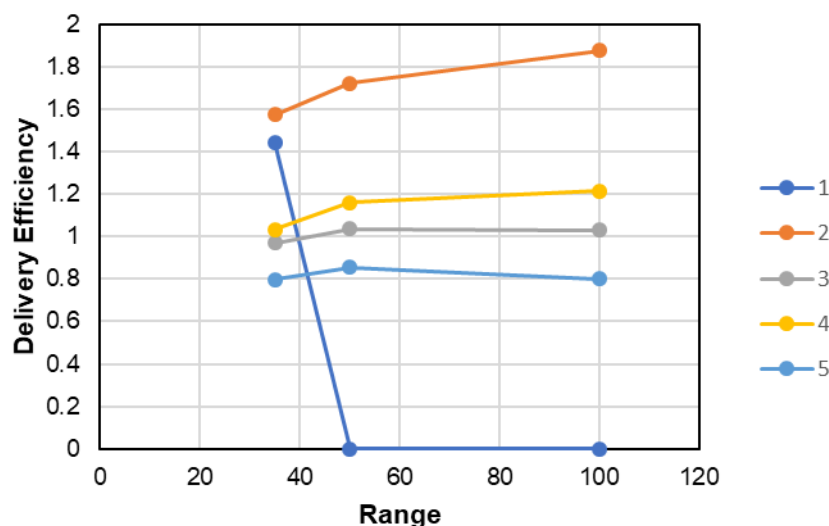


Figure 3.2-2 Productivity comparison of propulsion system architectures for varying mission distances.

suggests that convergence of battery-electric designs for longer mission ranges is highly sensitive to the wing weight estimation and the parameters which define the wing (lift coefficient, aspect ratio, etc).

4.0 CONCLUSION

This analysis of the scaling effects of various electric, mechanical, and hybrid propulsion systems showed that feasible solutions exist for a quad-rotor biplane tailsitter UAV to carry 5—50 lb of payload up to 100 nmi. For smaller payloads and shorter mission ranges, the battery-electric propulsion system resulted in the lightest GTOW design and also demonstrated the highest delivery efficiency. For the 50 lb payload delivery mission, the fuel-burning mechanical propulsion system configuration resulted in the lowest GTOW and highest delivery efficiency. The batter-electric configuration did not converge for 50 lb missions longer than 40 nmi. The convergence of the battery-electric designs are highly sensitive to the wing weight estimate from the physics-based methods. Fuel burning configurations showed a trend of significant increases in deliver efficiency for the larger payload while the battery-electric configuration only exhibited modest gains.

5.0 REFERENCES

- Avera, M. (2019). VTOL Concepts for Unmanned Payload Delivery Applications. *75th Vertical Flight Society Annual Forum*. Philadelphia, PA.
- EMRAX. (n.d.). *Technical Data and Manual for EMRAX Motors/Generators*. Retrieved 2019, from EMRAX: https://emrax.com/wp-content/uploads/2017/10/user_manual_for_emrax_motors.pdf
- Govindarajan, B., Sridharan, A., & Avera, M. (2017). Integration of Physics Based Weight Models into Rotorcraft Design Sizing. *42nd European Rotorcraft Forum*. Milan, Italy.
- Johnson, W. (2009). *NDARC - NASA Design and Analysis of Rotorcraft*. NASA - National Aeronautics and Space Administration.
- Leishman, J. G. (2006). In *Principles of Helicopter Aerodynamics* (pp. 115-170). Cambridge University Press.
- Lycoming. (n.d.). *EL-005 Engine*. Retrieved June 6, 2019, from Lycoming Engines: <https://www.lycoming.com/engines/el-005>
- Ng, W., Patil, M., & Datta, A. (2019). Hydrogen Fuel Cell and Battery Hybrid Architecture for Range Extension of Electric VTOL (eVTOL) Aircraft. *75th Annual Forum*. Philadelphia: Vertical Flight Society.
- Russell, C., Theodore, C., & Sekula, M. (2018). Incorporating Test Data for Small UAS at the Conceptual Design Level. *Technical Conference on Aeromechanics Design for Transformative Vertical Flight*. San Francisco, CA: American Helicopter Society.
- Singh, R., Sirohi, J., & Hrishikeshvan, V. (2019). Common Research Configuration for Collaborative Advancement of Scalable VTOL UAS Technologies. *75th Annual Forum*. Vertical Flight Society.
- Sridharan, A., Govindarajan, B., Nagaraj, V., & Chopra, I. (2016). Design Considerations of a Lift-Offset Single Main Rotor Compound Helicopter. *Aeromechanics Design for Vertical Lift Meeting*. San Francisco: American Helicopter Society.
- TRADOC. (2018). *The U.S. Army in Multi-Domain Operations 2028*. U.S. Army.
- US Army UAS Center of Excellence. (2010). *U.S. Army Roadmap for Unmanned Aircraft Systems 2010-2035*. Fort Rucker, AL.